Scientific Research Publishing

Atmospheric and Climate Sciences, 2026, 16(3), 557-575
https://www.scirp.org/journal/acs
ISSN Online: 2160-0422
ISSN Print: 2160-0414

Decadal Variability of Marine Atmospheric Boundary Layer over the Equatorial Atlantic and Its Impact on West African Rainfall

Modou Thioune*, Malick Wade, Mamadou Thiam, Cheikh Tidiane Déme

Laboratory of Atmospheric and Ocean Sciences-Materials, Energy and Devices (LSAO-MED), Gaston Berger University, Saint-Louis, Senegal
Email: *thioune.modou@ugb.edu.sn

How to cite this paper: Thioune, M., Wade, M., Thiam, M. and Déme, C.T. (2026) Decadal Variability of Marine Atmospheric Boundary Layer over the Equatorial Atlantic and Its Impact on West African Rainfall. *Atmospheric and Climate Sciences*, **16**, 557-575.
https://doi.org/10.4236/acs.2026.163028

Received: April 9, 2026
Accepted: May 23, 2026
Published: May 26, 2026

Abstract

This study analyses the decadal variability of the marine atmospheric boundary layer (MABL) in the equatorial Atlantic and its impact on the atmospheric circulation over West Africa. The study is based on data from the Simple Ocean Data Assimilation Ocean reanalysis, NCEP reanalyses and observations from the Climate Research Unit covering the period 1948-2008. We calculated the MABL index from potential temperature and analysed the mechanisms governing its variability using correlation and linear regression. The results reveal that the MABL is primarily governed by surface dynamic and thermodynamic forcings, in particular surface winds, sea surface temperature (SST) and its meridional gradient. The seasonal cycle shows MABL peaks in July-August-September, whilst the oceanic mixing layer and the SST gradient in September-October-November indicate a lag between atmospheric and oceanic anomalies associated with the cold tongue. Analysis of moving correlations and regression shows that the relationship between the MABL and oceanic and atmospheric parameters is not stationary. Before the early 1970s, variability in the MABL was primarily driven by local processes in the equatorial Atlantic, linked to SST gradients and thermocline dynamics. After this period, a shift in the climate regime becomes apparent, characterised by a weakening of equatorial temperature gradients and a growing influence of inter-basin teleconnections, particularly those associated with El Niño-Southern Oscillation. Variability in the MABL also appears to be linked to low-level atmospheric circulation and interactions with the West African monsoon. Before 1970, there was a strong positive precipitation anomaly across the entire Sahel, with maximum anomalies in the western part and negative anomalies in the regions around the Gulf of Guinea. In contrast, after 1970, negative anomalies began to appear in the western/coastal Sahel region. These results highlight the im-

portant role of the MABL in ocean-atmosphere coupling and the importance of improving the representation of lower-atmosphere processes in order to enhance future climate projections for West Africa.

Keywords

MABL, Decadal Variability, Teleconnexion, West African Monsoon

1. Introduction

Ocean-atmosphere interactions play a fundamental role in the variability of the climate system across all spatial and temporal scales. At the interface between these two environments, the marine atmospheric boundary layer (MABL) and the oceanic mixing layer (MLD) are key components of air-sea coupling. They control the exchange of sensible and latent heat, momentum and water vapor, thereby determining the boundary conditions that govern the evolution of meteorological and climatic systems [1] [2]. An accurate characterisation of their vertical structure and variability is crucial for improving the representation of surface processes in coupled models and enhancing climate predictability [3].

On a large scale, atmospheric dynamics are traditionally regarded as the primary driver of ocean variability. However, at meso-oceanic scales (10 - 200 km), the ocean actively influences the MABL through horizontal gradients in sea surface temperature (SST). Regions of strong thermal gradients associated with western boundary currents notably the Gulf Stream, the Kuroshio and the Agulhas Current constitute key zones of ocean-atmosphere interaction. *In situ* and satellite observations show that a positive SST anomaly is systematically associated with an intensification of surface winds, as well as with anomalies in divergence and rotational wind stress [4] [5].

Two main mechanisms have been proposed to explain this atmospheric response: 1) the Vertical Mixing Mechanism, according to which surface warming destabilises the MABL and promotes the vertical transfer of momentum [6], and 2) the Pressure Adjustment Mechanism, based on a hydrostatic adjustment linked to horizontal temperature gradients [7] [8]. These processes highlight the active role of SST fronts in the dynamic and thermodynamic organisation of MABL. Furthermore, some studies suggest that these anomalies may influence the free troposphere through the release of latent heat associated with convection, implying a possible impact on large-scale atmospheric circulation [9].

Beyond synoptic and seasonal scales, the MLD plays a key role in the climate system's thermal memory. SST anomalies that form in winter can be subducted beneath the seasonal mixing layer and re-emerge the following winter via the re-emergence mechanism [10] [11]. This process allows the ocean to exert an interannual influence on the atmosphere, despite the relatively short lifespan of surface anomalies [12] [13]. In mid-latitudes, the ocean accounts for around 20% of at-

mospheric variance, compared with 60% - 80% in the tropics, where ocean-atmosphere coupling is more intense [12]. The persistence of SST anomalies, modulated by the dynamics of the MLD, plays a central role in the manifestation and duration of these climate anomalies.

In West Africa, rainfall variability is strongly influenced by anomalies in Atlantic Sea surface temperature. Positive phases of the AMV (Atlantic Multidecadal Variability) are associated with a strengthening of the interhemispheric temperature gradient and a northward shift of the Intertropical Convergence Zone (ITCZ), leading to increased rainfall in Sahel, while negative phases correspond to the drought episodes observed in the 1970s and 1980s [14] [15]. This link can be expressed both indirectly, through changes in general circulation, and directly, through the influence of the SST on the stability of the MABL, evaporation and convection in the tropical Atlantic.

Despite the significant progress made in recent decades, a number of uncertainties remain regarding the relative importance of the dynamic and thermodynamic mechanisms linking variability in the MABL and MLD to precipitation anomalies in West Africa. In this context, this paper aims to analyse the decadal variability of the MABL and impact on atmospheric circulation over Equatorial Atlantic, as well as on rainfall over West Africa.

The paper is organised as follows: Section 2 describes the data used and the analytical methods employed. Section 3 presents the results, accompanied by a discussion, concerning the variability of the marine atmospheric boundary layer and its relationship with sea surface temperatures, winds, surface pressures and precipitation in West Africa. Section 4 is devoted to the conclusion, which summarizes the main findings and perspectives for future research.

2. Data and Methods

2.1. Data

In this study, we use version 2.2.4 of the Simple Ocean Data Assimilation (SODA 2.2.4) reanalyses [16]. This version corresponds to their first assimilation simulation spanning over 100 years and utilises wind data from the 20Crv2 satellite. The ocean model is based on the Parallel Ocean Program (POP) physics, with an average resolution of $0.25^\circ \times 0.4^\circ$ over 40 levels. The observational data include in-situ and satellite data. The results are presented as monthly averages, projected onto a uniform grid of $0.5^\circ \times 0.5^\circ \times 40$ levels covering 1901-2008 period. Data are available for download:
https://www.cen.uni-hamburg.de/en/icdc/data/ocean/easy-init-ocean/soda-224.htm.

Observational data from the Hadley Centre Sea Ice and Sea Surface Temperature (HadISST) are also used. This dataset includes a combination of complete global monthly fields of SST and sea ice concentration on a $1^\circ \times 1^\circ$ latitude-longitude grid, from 1870 to the present day [17]. HadISST1 data are compiled from SST measurements derived mainly from ship-based observations and, since 1982,

from a combination of *in situ* measurements and satellite-derived SSTs. The dataset can be accessed and downloaded: https://www.metoffice.gov.uk/hadobs/hadisst/data/download.html.

We also used observed precipitation data from the Climate Research Unit Time Series (CRU TS). CRU TS is a monthly 0.5˚ × 0.5˚ grid-based terrestrial climate dataset available from 1901 onwards and covering all land areas except Antarctica [18]. It is based on the interpolation of monthly climate anomalies derived from an extensive network of weather stations. In the CRU TS v4 version, the station time series are first converted into anomalies relative to the 1961-1990 period, and then interpolated using angular distance weighting. The interpolated anomalies are then converted into actual climate values using the CRU CL v1.0 climatologies. The data are publicly available for download: https://crudata.uea.ac.uk/cru/data/hrg/.

Reanalyses from the National Centers for Environmental Prediction (NCEP) in collaboration with the National Center for Atmospheric Research (NCAR), known as the NCEP/NCAR Reanalysis, were also used to calculate the MABL. They cover the period from 1948 to present with a monthly temporal resolution. The data are provided on a global grid of 2.5˚ × 2.5˚ (longitude × latitude) and comprise 17 pressure levels ranging from 1000 to 10 hPa. Data are available for download: https://apdrc.soest.hawaii.edu/datadoc/ncep_mon.php.

2.2. Methods

2.2.1. Marine Atmospheric Boundary Layer Height

In this study, the MABL top is defined as the altitude where the gradient of the potential temperature between 700 and 2500 m is maximal as in [19]. This involves identifying the altitude at which the potential (or virtual) temperature gradient is at its maximum, marking the transition between the turbulent layer and the free atmosphere [20] [21]. The MABL index is then constructed by spatially averaging the MABL over the equatorial Atlantic region (20˚W - 5˚W, 2˚N - 4˚S) and finally standardized.

2.2.2. Mixed Layer Depth and Thermocline Depth

Oceanic MLD relies primarily on two main categories of methods: threshold methods and gradient methods. In this study, the method based on a density threshold of 0.03 Kg m/m^2 is used as it provides a better estimate of the MLD [22] [23]. The depth of the surface mixing layer is defined as the depth z at which the potential density difference $\Delta\sigma_\theta(z)=\sigma_\theta(z)-\sigma_\theta(z_0)$ in the upper ocean exceeds a specified threshold value. Here z_0 is a reference depth (generally in the range $z_0=0$ at the ocean surface to 10 m), and $\sigma_\theta(z)=\rho_\theta(z)-1000$ Kg·m^{-3} is the density anomaly for the measured potential density ρ_θ.

Thermocline depth (THD) is estimated from the 20˚C isotherm using data from the SODA dataset. This approach is based on the assumption that the 20˚C isotherm is a good proxy for the thermocline position in tropical regions [24].

2.2.3. Statistical Tools

1) Anomaly

An anomaly calculation involves measuring the deviation of a variable from a reference value, often a climatological mean. By subtracting the long-term mean from the observed value, an anomaly is obtained, which facilitates comparisons between different periods and the analysis of trends or extreme events. Anomalies are calculated by removing the monthly climatology from each variable in order to eliminate the seasonal cycle. A detrending procedure is then applied to the anomalies to remove long-term trends that could influence the analyses. Finally, the same reference period (1948-2008) is used for all the variables considered.

$$A_t = X_t - \overline{X}_{ref} \tag{1}$$

A_t is the anomaly,

X_t is the observed value,

$\overline{X}_{ref}$ is the climatological mean over the reference period (1948-2008).

2) Correlation and Linear Regression

The 20-year moving correlation between oceanic and atmospheric parameters allows us to examine how interactions between the ocean and the atmosphere evolve over time. It highlights slow variations, regime shifts, and the strengthening or weakening of climatic links. This approach thus provides a dynamic view of ocean-atmosphere interactions, which is essential for understanding long-term climate variability and anticipating its impacts [25]. In this study, we use Pearson's correlation coefficient based on the following estimator [26].

$$r_t = \frac{\sum_{i=t-\omega+1}^{t}\left(x_i - \overline{x}_t\right)\left(y_i - y_t\right)}{\sqrt{\sum_{i=t-\omega+1}^{t}\left(x_i - \overline{x}_t\right)^2}\sqrt{\sum_{i=t-\omega+1}^{t}\left(y_i - \overline{y}_t\right)^2}} \tag{2}$$

where:

r_t is the moving correlation at time t

ω is the window size (number of observations),

x are y two independent variables,

$\overline{x}_t$ is the mean of x over the window,

$\overline{y}_t$ is the mean of y over the same window.

The regression is the slope given by:

$$\hat{\beta}_1 = \frac{\sum_{i=1}^{n}\left(x_i - \overline{x}\right)\left(y_i - \overline{y}\right)}{\sum_{i=1}^{n}\left(x_i - \overline{x}\right)^2} \tag{3}$$

A 20-year moving window is used to analyze the temporal evolution of relationships by computing statistics over successive overlapping sub-periods, thereby revealing low-frequency variability and the non-stationarity of the processes [27]-[29]. The first period (1948-1971) contains 24 points and the second period (1972-2008) contains 37 points.

The statistical significance of the results is assessed using appropriate statistical tests. For moving correlations and linear regressions, a bootstrap procedure based on a Monte Carlo technique involving 300 permutations is applied. Only results

that are statistically significant at the 95% confidence level are retained.

3. Results and Discussion

3.1. Seasonal Cycle in the Equatorial Atlantic

Figure 1 shows the seasonal cycle of the MABL height, the MLD depth and the SST gradient. The MABL remains relatively stable between January and May (700 - 750 m), a period characterised by more stable atmospheric stratification, indicating low turbulent flux between the ocean and the atmosphere [30] [31]. From June MABL rises rapidly, reaching a maximum of around 1100 m in August. This trend is preceded by a decrease in the SST gradient, which reaches its minimum in July, suggesting a time lag of around one month between changes in SST and the response of the MABL. Indeed, the reduction in the SST gradient promotes cooling of the ocean surface and an increase in turbulent heat fluxes to the atmosphere, thereby enhancing instability and the thickening of the MABL [2] [4] [32].

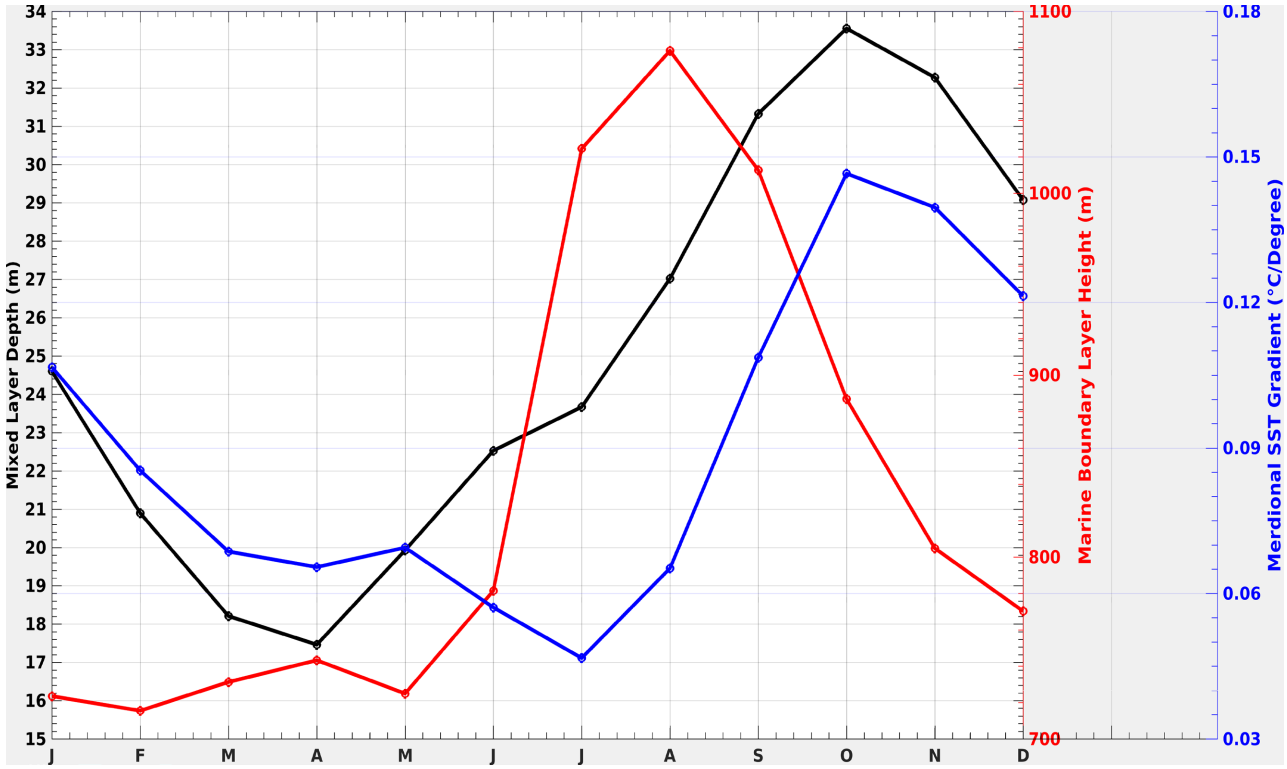

Figure 1. Seasonal cycle of MABL, MLD, gradySST (averaged between 20˚W - 5˚W, 2˚N - 4˚S).

The MLD reaches a minimum in April (17 m) and a maximum in October (34 m). From April to October, its gradual deepening is consistent with the increase in heat flux, and thus a strengthening of the surface wind and the development of Atlantic cold tongue consistent with the work of [33]-[35]. Between October and April, there is a decrease in the MLD; this decrease is likely linked to a weakening of the southerly wind and a reduction in vertical mixing (thin MABL), as suggested by [36].

3.2. Moving Average of the MABL and the MLD

Figure 2 shows the trend in the 20-year moving average of MABL height and MLD during the JJA season in the Equatorial Atlantic Cold Water Tongue region (20˚W - 5˚W; 4˚S - 2˚N) for the 1948-2008 period. The use of a moving average makes it possible to filter out interannual variability and highlight low-frequency climatic fluctuations associated with ocean-atmosphere interactions in tropical regions [37] [38]. Over 1948 to the mid-1950s period, MLD was slightly positive whilst the MABL remained relatively stable, indicating a relatively balanced state of the ocean-atmosphere system in the equatorial cold tongue. Between the mid-1950s and the mid-1960s, variability remained moderate, with positive fluctuations in the MABL while the MLD gradually decreased, possibly due to variations in the intensity of the equatorial trade winds. A clearly negative phase then emerges between the mid-1960s and the early 1970s, a period during which both variables reach their lowest values. Stronger stratification limits vertical mixing and results in a thinner mixing layer [33] [39], and sea surface cooling stabilises the atmospheric boundary layer and reduces its thickness [2] [4]. From the early 1970s, both variables show an upward trend. The period 1973-1980 corresponds to a transitional phase characterised by a gradual rise towards less negative values, possibly linked to a weakening of upwelling and a relative warming of the ocean surface. In 1980s, the MABL increased more sharply and the MLD returned to positive values.

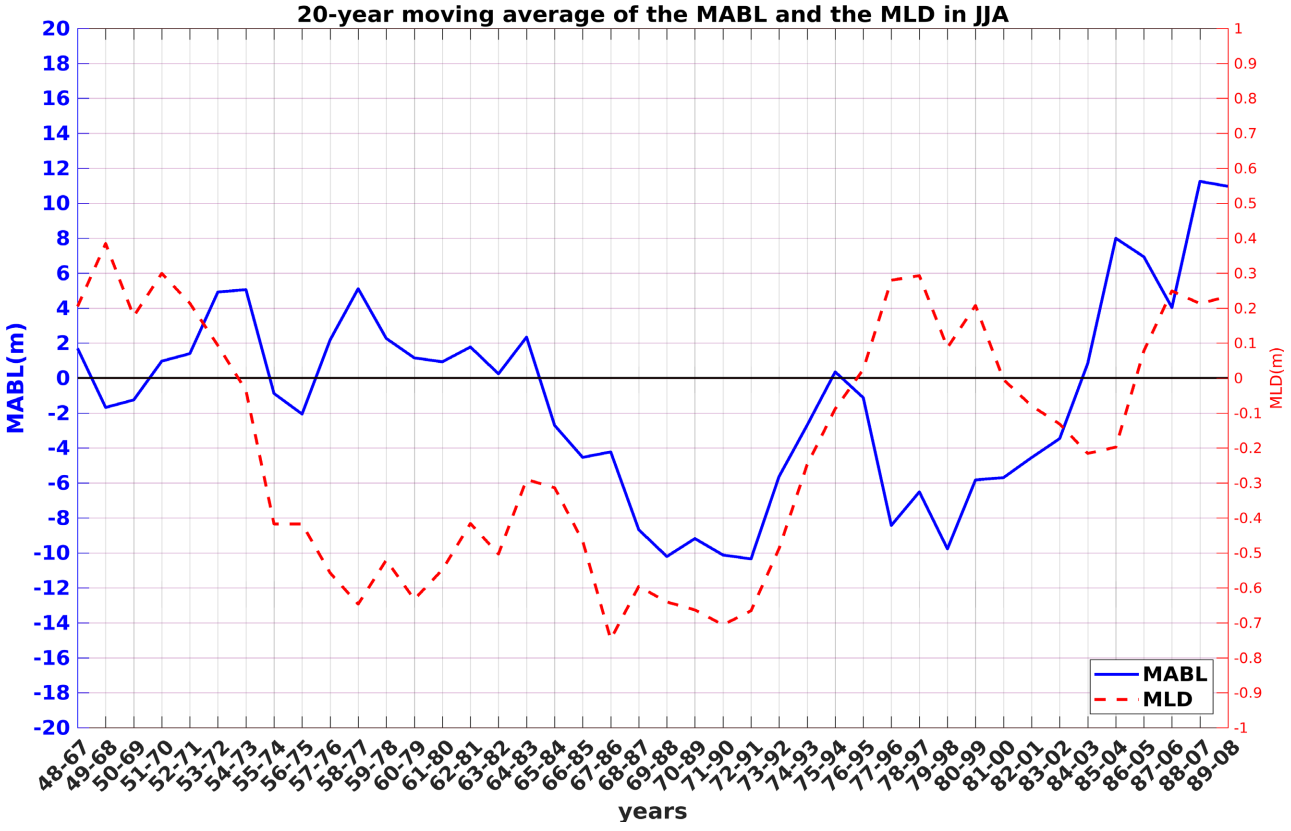

Figure 2. 20-year moving average of the MABL and the MLD (averaged between 20˚W - 5˚W, 2˚N - 4˚S).

We will now examine the mechanisms that govern the decadal variability of the MABL. Figure 3 shows the temporal evolution of the moving correlations between MABL height and several atmospheric and oceanic parameters over the period 1948-2008. The indices are averaged over the equatorial cold-water tongue region of the Atlantic, bounded by 2˚N - 4˚S and 20˚W - 5˚W. Moving correlations are calculated using a 20-year time window in order to analyse long-term variability. The analysis is restricted to the JJA season. This approach allows the identification of dominant relationships as well as any long-term variations therein.

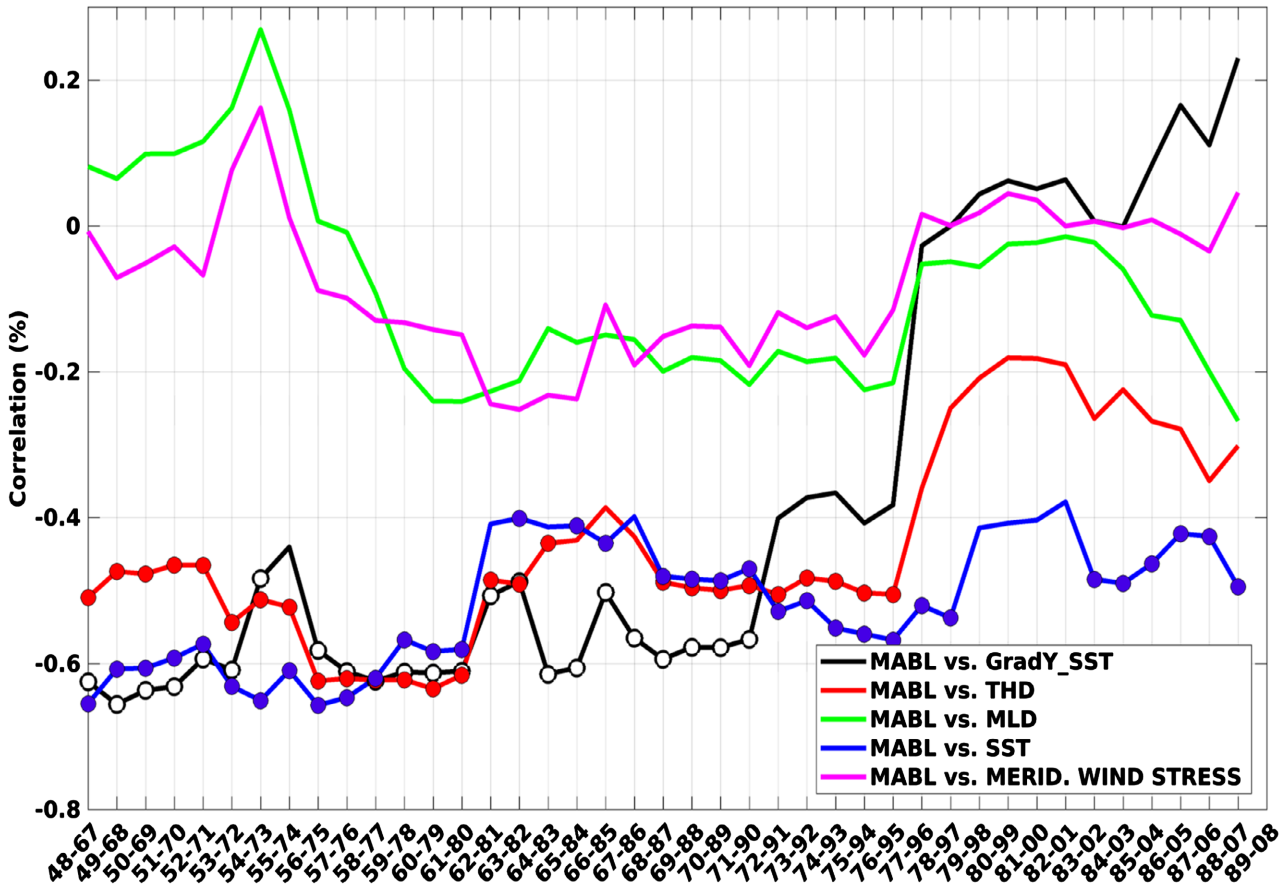

Figure 3. 20 years-moving correlation between MABL and MLD, SST, SST gradient, and meridional wind THD over Equatorial Atlantic (averaged between 20˚W - 5˚W, 2˚N - 4˚S. Circles indicate statistically significant correlation at 95% confidence level.

Over the entire period, weak and non-significant positive correlations were observed between MABL and MLD, as well as between the MABL and the meridional wind (V). These results suggest that the influence of surface ocean dynamics and meridional circulation on the MABL is not direct, but occurs via other variables, particularly thermodynamic ones, such as SST and air-sea turbulent fluxes [2] [32].

By contrast, the correlation between MABL and SST is generally negative and significant throughout the entire period studied, with the exception of a few in-

tervals where it is weaker and non-significant. This persistent link highlights the fundamental role of SST in controlling the stability and vertical structure of the MABL, particularly through turbulent heat fluxes, as suggested by [4] [5].

However, the relationship between the MABL, the meridional SST gradient (dSST/dy) and the thermocline (THD) is non-stationary. Indeed, while the correlations between the MABL and dSST/dy, as well as between the MABL and THD, were negative and significant during the period 1948-1971, they became positive and insignificant from in 1970. These temporal breaks suggest the existence of a climate regime shift affecting air-sea coupling mechanisms. Such changes are consistent with the large-scale climatic reorganisations documented in the 1970s, notably the climate shift of 1976-1977, which is largely associated with lasting changes in atmospheric and oceanic circulation in tropical and subtropical basins [40]-[42]. These reorganisations may have altered the structure of oceanic temperature gradients, the intensity of air-sea fluxes and, consequently, the sensitivity of the MABL to local thermodynamic forcings.

In summary, if MABL variability was strongly controlled by local mechanisms in the equatorial Atlantic notably dSST/dy and THD prior to the 1970s, this variability appears to have been driven by remote factors from 1970 onwards. The weakening of the correlations between the MABL and the SST gradient or THD after the 1970s suggests a transition towards a regime in which the MABL is more strongly controlled by large-scale atmospheric forcings [43] [44]. In the next section, we will attempt to understand the climate shift through SST signals across the two periods.

3.3. Global Sea Surface Temperature Anomalies Associated with Decadal Variability in the Sea Surface Temperature

Figure 4 displays the regression fields for SST anomalies associed to the depth-based MABL index (see the Methods section for details on how the index is calculated) for two distinct periods: 1948-1971 and 1972-2008.

Over the period 1948-1971, a significant cooling was observed across the entire equatorial Atlantic, with the greatest cooling occurring along the equatorial cold-water tongue, and a barely significant warming in the northern tropical Atlantic. These anomalies form an SST dipole in the tropical Atlantic associated with the Atlantic Meridional Mode, as described by [45]. Negative SST anomalies peak at lags −1 and 0 (MJJ and JJA); this corresponds to the phase of intensification of the cold tongue. During this season, the southerly trade winds promote the upwelling of the thermocline and strengthen upwelling in the eastern Atlantic, leading to a cooling of surface waters and amplifying negative SST anomalies [46] [47]. In the Pacific, negative SST anomalies are appearing across the entire equatorial Pacific; this anomaly becomes significant from lag −4, well after the negative anomaly in the Tropical Atlantic: the MABL variability is driven by the SST gradient in the Tropical Atlantic (the meridional mode), hence the strong correlation between the MABL and the meridional SST gradient during this period (see **Figure 3**).

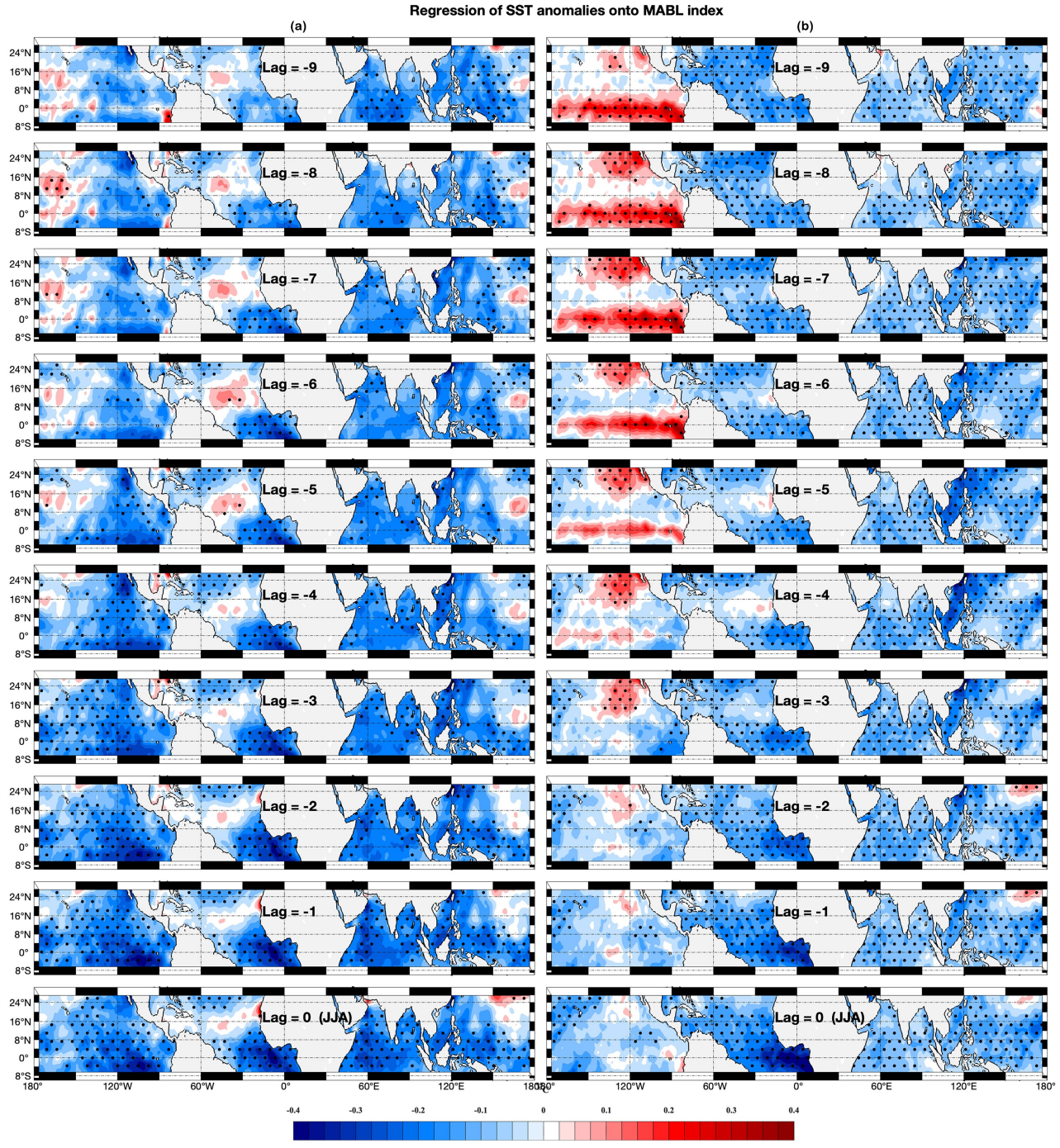

Figure 4. Linear regression of the SST on the MABL index. Black dots represent areas that are statistically significant at 95% confidence level. (a) 1948-1971, (b) 1972-2008.

By contrast, over the period 1972-2008, the MABL is evident across all basins: the tropical Atlantic, the Indian Ocean and also the Pacific. The pattern of SST anomalies shows a notable change: significant positive anomalies of around 0.4˚C appear in the tropical Pacific, between lag −9 and lag −6, peaking at lag −8. This SST pattern is associated with the warm phase of El Niño-Southern Oscillation (ENSO), El Niño in the Pacific, which, according to the literature, began to be-

come significant from the 1970s [48]. In the equatorial Atlantic, the negative SST anomaly still appears, but this anomaly is at its maximum at lag 0 in JJA. ENSO-related SST anomalies alter tropical convection and the structure of global atmospheric circulation, notably the Walker circulation [49] [50].

In summary, the difference observed between the two periods can be interpreted as a shift in the tropical climate regime that occurred around the 1970s. After the 1970s, the influence of the Pacific on the tropical Atlantic appears to have become more pronounced, which would explain the presence of a precursor ENSO signal in the Pacific prior to the development of the cold tongue in the Atlantic. Regression analysis of SSTs against the MABL index reveals a change in ocean-atmosphere coupling in the equatorial Atlantic between the two periods studied. Prior to 1970, the variability of the MABL, or the equatorial cold-water tongue, appears to have been dominated by local processes linked to the ocean-atmosphere dynamics of the equatorial Atlantic, namely the meridional mode. By contrast, after 1970, the variability of the cold tongue appears to be more strongly influenced by teleconnections associated with ENSO, suggesting a stronger interaction between the two tropical basins. In the following sections, we will analyse the atmospheric dynamics associated with MABL variability and its impact on rainfall in West Africa.

3.4. Atmospheric Circulation in the Tropical Atlantic

Figure 5 shows the regression of wind speed, wind direction and mean sea-level pressure (MSLP) anomalies on the MABL index over 1948-1971 and 1972-2008 periods. Remember that negative lags indicate that atmospheric anomalies lead MABL variability and positive when these anomalies lag the MABL index.

Over the period 1948-1971 (**Figure 5(a)**), an increase in wind tension is observed north of 16˚N. This anomaly, which appears two months before the peak of MABL variability (lag −2), is driven by positive MSLP anomalies and may be associated with the southern part of the Azores High.

Between 8˚N and 16˚N, offshore, the wind anomaly is negative, reflecting a weakening of the northeasterly trade winds. In contrast, the southeasterly trade winds strengthen north of the equator (between 15˚N and 30˚N) as one approaches lag 0, then persist for a month afterward (lag+1). This strengthening can be explained by a dipole of MSLP anomalies: negative north of the equator and positive south of it. The negative MSLP anomaly, near the continent, promotes the inflow of a westerly flow toward the West African continent, while the positive anomaly generates a southward wind anomaly in the cold tongue region, reflecting a decrease in the monsoon flow which disappears entirely at lags 0 and +1.

Over the 1972-2008 period (**Figure 5(b)**), which the exception of a signal indicating a weakening of the Azores High north of 16˚N (in contrast to the previous period, where a strengthening was observed), the structures of wind and MSLP anomalies remain broadly similar. However, the westerly flow is less intense, and the decrease in the monsoon flow is significantly more pronounced.

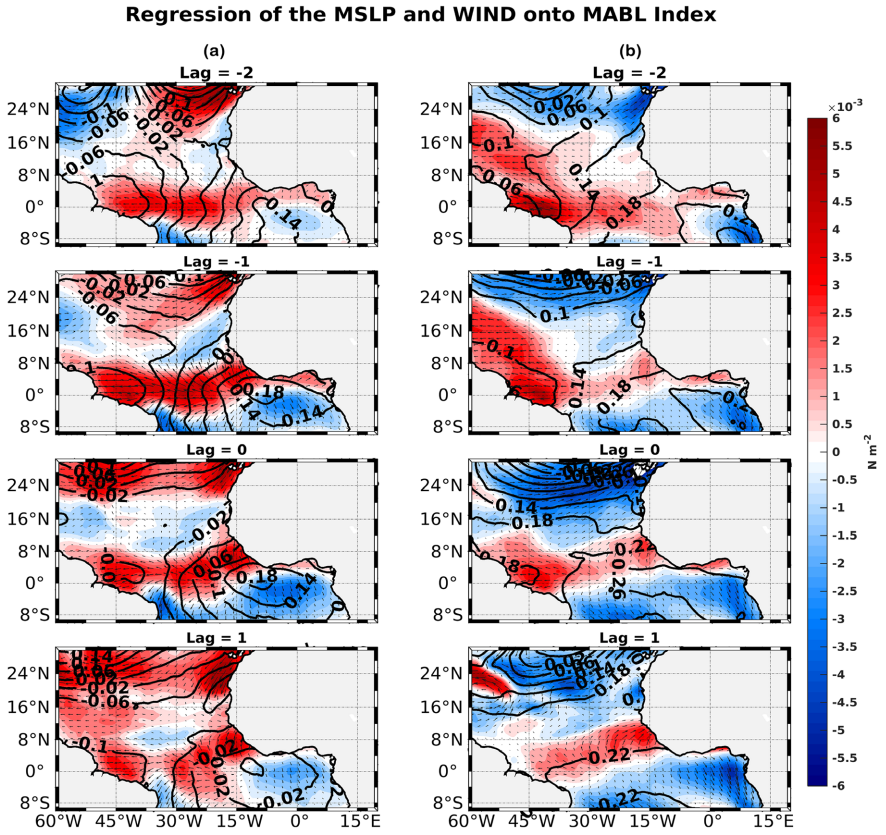

Figure 5. Linear regression of stress wind (colors and vectors) and MSLP (contours) anomalies on the MABL index for 1948-1971 period (a) and 1972-2008 period (b). Only MSLP anomalies significant at 95% confidence level are shown.

3.5. Impact on Rainfall in West Africa

To examine the precipitation signals associated with MABL variability, we present in **Figure 6** a regression of precipitation anomalies in West Africa against the MABL index for two distinct periods (1948-1971 and 1972-2008).

Across both periods, a dipole pattern of precipitation anomalies is observed: positive over the Sahel and negative over the Gulf of Guinea region. The increase in precipitation over the Sahel can be explained by the strengthening of the south-easterly trade winds as well as a more intense westerly flow, while the decrease observed over the Gulf of Guinea is linked to a weakening of the southwesterly monsoon flow. However, significant differences emerge between the two periods. The dipole is much more pronounced during the 1948-1971 period than during 1972-12008, and clearly opposite anomalies are observed over the western Sahel. Indeed, during 1948-1971, a maximum positive anomaly is observed over the coastal areas of the Sahel, whereas it becomes negative during 1972-2008. This maximum positive anomaly can be attributed to the strengthening of the westerly flow, which constitutes the main source of moisture for precipitation in the western Sahel [51] [52]. In contrast, during 1972-2008, the precipitation anomaly becomes negative in this same region, while it remains positive over the rest of the Sahel.

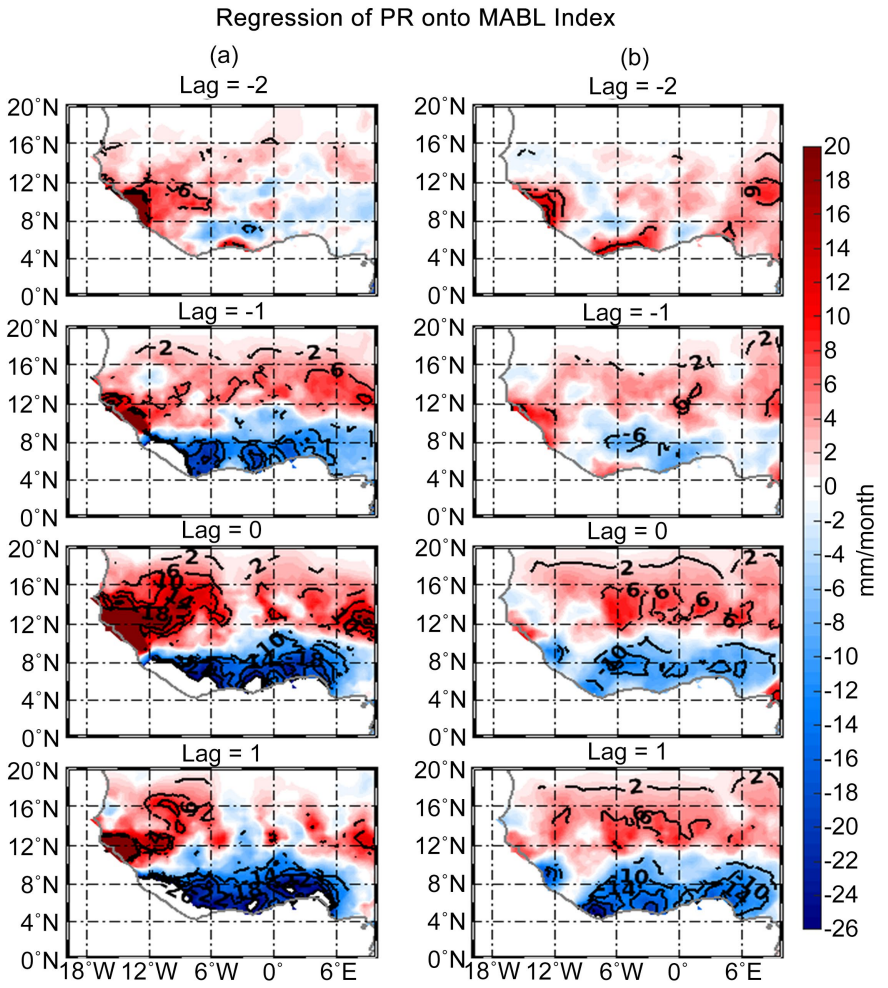

Figure 6. Linear regression of precipitations anomalies on the MABL index for 1948-1971 period (a) and 1972-2008 period (b). The black contours indicate anomalies that are statistically significant at 95% confidence level.

4. Conclusions

We study the decadal variability of the MABL over the equatorial Atlantic. Using observational data from the CRU and SODA and NCEP reanalyses, we examine the different atmospheric and oceanic mechanisms that govern this variability and its impact on summer rainfall in West Africa over the 1948-2008 period.

We then focused on the JJA season, during which the index exhibits its maximum variability.

The 20 years-moving correlation between anomalies in oceanic and atmospheric parameters and the MABL reveal non-stationarity relationships between the MABL and these anomalies. Before 1970, strong and significant negative correlations between MABL meridional gradient of STT and THD over Equatorial Atlantic (averaged between 20˚W - 5˚W, 2˚N - 4˚S) indicate a marked local control of these parameters on the MABL, likely through turbulent fluxes that destabilize the atmosphere and promote its thickening. After 1970, correlations weaken and become statistically non-significant, suggesting a stronger influence of large-

scale forcing on atmospheric variability and a reduction in local-scale interactions. In contrast, the MABL/SST relationship remains nearly stationary, negative, and significant throughout the period (with the exception of a few years). We will then attempt to understand why the mechanisms governing MABL variability have changed by conducting a composite analysis over the two periods: 1948-1971 and 1972-2008.

The regression analysis of sea surface temperature anomalies onto the MABL index reveals significant differences between the two periods, which may explain the shift in the mechanisms governing MABL variability. Between 1948 and 1971, this variability was mainly dominated by local processes in the equatorial Atlantic, associated with the meridional mode and the intensification of the cold tongue. During boreal summer (JJA), the cooling of SSTs (−0.4˚C) in the equatorial Atlantic results from the strengthening of southeast winds, which enhances the release of turbulent fluxes, destabilizes the atmosphere and promotes a particularly deep MABL. Conversely, the Atlantic Niño phenomenon warms SSTs, which strengthens convection, weakens the northeasterly winds, and further enhances atmospheric instability. After the 1970s, the influence of inter-basin teleconnections becomes more pronounced, with a significant role of the El Niño-Southern Oscillation (which peaks at about +0.4˚C in boreal winter) in modulating SST anomalies over Equatorial Atlantic, consistent with [53], who noted a shift from SST control to ENSO after the 1960s. This suggests a strengthening of Atlantic-Pacific teleconnexion in tropical climate variability. During an El Niño event, warming in the equatorial Pacific shifts convection eastward, enhancing upward motion in that region. As compensation, subsidence develops over the equatorial Atlantic, stabilizing the atmosphere and reducing convection.

To understand the dynamics, we performed a linear regression of wind speed, wind direction and MSLP anomalies on the MABL index. The results show changes in atmospheric circulation over tropical Atlantic between these two periods. During the first period (1948-1971), a strengthening of the Azores High is observed north of 16˚N, associated with a dipole of sea-level pressure anomalies between the northern and southern hemispheres, along with a weakening of the northeasterly trade winds. Near the West African coast, a strengthening of the westerly flow from the eastern Atlantic toward the continent is also observed, together with a weakening of the monsoon flow originating south of the equator. The North-South and ocean-continent pressure dipole primarily modulates the intensity of the southeasterly trade winds. During the second period, although the Azores High weakens, the westerly flow toward the continent is also less intensified compared to the first period. This confirms that the strengthening of the westerly flow observed during the first period is not directly related to large-scale dynamics, particularly to the Azores High. However, the monsoon flow becomes weaker, reaching its maximum weakening at lag 1, corresponding to approximately one month after the peak of MABL variability.

The analysis of West African precipitation anomalies in relation to this variability reveals a rainfall dipole between the Sahel and the Gulf of Guinea regions.

This dipole is more pronounced during the 1948-1971 period than during 1972-2008. The decrease in precipitation during the latter period may be linked to the positive phase of ENSO, which, according to [48], reduces rainfall over the Sahel through the warming of the equatorial Atlantic and Pacific/Indian Oceans. The rainfall contrast between the Sahel and the Gulf of Guinea can be explained by a reorganization of low-level circulation, controlled by pressure gradients and ocean-atmosphere interactions in the tropical Atlantic. The strengthening of the southeasterly trade winds and the weakening of the northeasterly trades favor a northward shift of the ITCZ, as well as a more pronounced westerly flow toward the continent, which helps explain the enhanced rainfall over the Sahel. This process is driven by a stronger North-South pressure gradient, associated with lower pressure near the coast and higher pressure over the Atlantic. This configuration intensifies low-level winds and moisture advection toward the Sahel [52] [54]. In contrast, it induces relative divergence over the Gulf of Guinea. The negative wind stress anomaly observed in the south weakens the southeasterly trade winds, leading to a decrease in precipitation in this region. Both periods exhibit a rainfall dipole, with increased precipitation over the Sahel and reduced precipitation over the Gulf of Guinea, but this contrast is stronger during 1948-1971. During this first period, the western Sahel is particularly wet due to a strengthened westerly flow, whereas in 1972-2008 it becomes drier, despite still-positive anomalies over the rest of the Sahel, reflecting a redistribution of moisture toward the coastal Sahelian band.

This study opens several perspectives, including a deeper investigation of the dynamical processes linking the MABL to precipitation, particularly air-sea fluxes and atmospheric stability. It would also be relevant to assess the ability of climate models, such as CMIP6, to reproduce this variability and its impacts on circulation in the tropical Atlantic and West Africa. Moreover, incorporating intra-seasonal timescales would allow for a better characterization of the variability of the marine boundary layer and help understand the mechanisms through which the ocean responds to this variability over the equatorial Atlantic. However, this present study has allowed us to better understand the long-term variability of the marine boundary layer and its role in rainfall variability in West Africa.

Acknowledgements

This work was supported by the Laboratoire Mixte Internatinale (LMI-ECLAIRS2). This study benefited computing resource of Centre d'Excellence africain en Mathématiques, Informatique et TIC (CEA-MITIC) at Gaston Berger University.

Authors Contributions

Modou Thioune: Conceptualization, methodology, investigation, visualization, writing—original draft, writing—review.

Prof. Malick Wade: Conceptualization, resources, supervision, methodology, investigation, formal analysis, validation, writing—review & editing.

Dr. Mamadou Thiam: Supervision, methodology, investigation, formal analy-

sis, validation, writing—review & editing.

Cheikh Tidiane Déme: Investigation, formal analysis, writing—review & editing.

Conflicts of Interest

The authors declare no conflicts of interest regarding the publication of this paper.

References

[1] Gill, A.E. (1982) Studies of Moisture Effects in Simple Atmospheric Models: The Stable Case. *Geophysical & Astrophysical Fluid Dynamics*, **19**, 119-152. https://doi.org/10.1080/03091928208208950

[2] Small, R.J., deSzoeke, S.P., Xie, S.P., O'Neill, L., Seo, H., Song, Q., *et al.* (2008) Air-Sea Interaction over Ocean Fronts and Eddies. *Dynamics of Atmospheres and Oceans*, **45**, 274-319. https://doi.org/10.1016/j.dynatmoce.2008.01.001

[3] Zhai, X., Wu, S., Liu, B., Song, X. and Yin, J. (2018) Shipborne Wind Measurement and Motion-Induced Error Correction of a Coherent Doppler Lidar over the Yellow Sea in 2014. *Atmospheric Measurement Techniques*, **11**, 1313-1331. https://doi.org/10.5194/amt-11-1313-2018

[4] Chelton, D.B., Schlax, M.G., Freilich, M.H. and Milliff, R.F. (2004) Satellite Measurements Reveal Persistent Small-Scale Features in Ocean Winds. *Science*, **303**, 978-983. https://doi.org/10.1126/science.1091901

[5] Xie, S. (2004) Satellite Observations of Cool Ocean-Atmosphere Interaction. *Bulletin of the American Meteorological Society*, **85**, 195-208. https://doi.org/10.1175/bams-85-2-195

[6] Sweet, W., Fett, R., Kerling, J. and La Violette, P. (1981) Air-Sea Interaction Effects in the Lower Troposphere across the North Wall of the Gulf Stream. *Monthly Weather Review*, **109**, 1042-1052. https://doi.org/10.1175/1520-0493(1981)109<1042:asieit>2.0.co;2

[7] Hsu, S.A. (1984) Sea-Breeze-Like Winds across the North Wall of the Gulf Stream: An Analytical Model. *Journal of Geophysical Research*: *Oceans*, **89**, 2025-2028. https://doi.org/10.1029/jc089ic02p02025

[8] Lindzen, R.S. and Nigam, S. (1987) On the Role of Sea Surface Temperature Gradients in Forcing Low-Level Winds and Convergence in the Tropics. *Journal of the Atmospheric Sciences*, **44**, 2418-2436. https://doi.org/10.1175/1520-0469(1987)044<2418:otross>2.0.co;2

[9] Minobe, S., Kuwano-Yoshida, A., Komori, N., Xie, S. and Small, R.J. (2008) Influence of the Gulf Stream on the Troposphere. *Nature*, **452**, 206-209. https://doi.org/10.1038/nature06690

[10] Alexander, M.A. and Deser, C. (1995). A Mechanism for the Recurrence of Wintertime Midlatitude SST Anomalies. *Journal of Physical Oceanography*, **25**, 122-137. https://journals.ametsoc.org/view/journals/phoc/25/1/1520-0485_1995_025_0122_amftro_2_0_co_2.xml

[11] Cassou, C., Deser, C. and Alexander, M.A. (2007) Investigating the Impact of Reemerging Sea Surface Temperature Anomalies on the Winter Atmospheric Circulation over the North Atlantic. *Journal of Climate*, **20**, 3510-3526. https://doi.org/10.1175/jcli4202.1

[12] Kushnir, Y., Robinson, W.A., Bladé, I., Hall, N.M.J., Peng, S. and Sutton, R. (2002)

Atmospheric GCM Response to Extratropical SST Anomalies: Synthesis and Evaluation*. *Journal of Climate*, **15**, 2233-2256. https://doi.org/10.1175/1520-0442(2002)015<2233:agrtes>2.0.co;2

[13] Namias, J. and Born, R.M. (1970) Temporal Coherence in North Pacific Sea-Surface Temperature Patterns. *Journal of Geophysical Research*, **75**, 5952-5955. https://doi.org/10.1029/jc075i030p05952

[14] Folland, C.K., Palmer, T.N. and Parker, D.E. (1986) Sahel Rainfall and Worldwide Sea Temperatures, 1901-85. *Nature*, **320**, 602-607. https://doi.org/10.1038/320602a0

[15] Rowell, D.P. (2003) The Impact of Mediterranean SSTs on the Sahelian Rainfall Season. *Journal of Climate*, **16**, 849-862. https://doi.org/10.1175/1520-0442(2003)016<0849:tiomso>2.0.co;2

[16] Giese, B.S. and Ray, S. (2011) El Niño Variability in Simple Ocean Data Assimilation (SODA), 1871-2008. *Journal of Geophysical Research*, **116**, C02024. https://doi.org/10.1029/2010jc006695

[17] Rayner, N.A., Parker, D.E., Horton, E.B., Folland, C.K., Alexander, L.V., Rowell, D.P., *et al.* (2003) Global Analyses of Sea Surface Temperature, Sea Ice, and Night Marine Air Temperature since the Late Nineteenth Century. *Journal of Geophysical Research*: *Atmospheres*, **108**, D14. https://doi.org/10.1029/2002jd002670

[18] Harris, I., Osborn, T.J., Jones, P. and Lister, D. (2020) Version 4 of the CRU TS Monthly High-Resolution Gridded Multivariate Climate Dataset. *Scientific Data*, **7**, Article No. 109. https://doi.org/10.1038/s41597-020-0453-3

[19] Leduc-Leballeur, M., Eymard, L. and de Coëtlogon, G. (2011) Observation of the Marine Atmospheric Boundary Layer in the Gulf of Guinea during the 2006 Boreal Spring. *Quarterly Journal of the Royal Meteorological Society*, **137**, 992-1003. https://doi.org/10.1002/qj.808

[20] Hashizume, H., Xie, S., Fujiwara, M., Shiotani, M., Watanabe, T., Tanimoto, Y., *et al.* (2002) Direct Observations of Atmospheric Boundary Layer Response to SST Variations Associated with Tropical Instability Waves over the Eastern Equatorial Pacific. *Journal of Climate*, **15**, 3379-3393. https://doi.org/10.1175/1520-0442(2002)015<3379:dooabl>2.0.co;2

[21] Wayland, R.J. and Raman, S. (1989) Mean and Turbulent Structure of a Baroclinic Marine Boundary Layer during the 28 January 1986 Cold-Air Outbreak (GALE 86). *Boundary-Layer Meteorology*, **48**, 227-254. https://doi.org/10.1007/bf00158326

[22] Lee, C.M., Jones, B.H., Brink, K.H. and Fischer, A.S. (2000) The Upper-Ocean Response to Monsoonal Forcing in the Arabian Sea: Seasonal and Spatial Variability. *Deep Sea Research Part II*: *Topical Studies in Oceanography*, **47**, 1177-1226. https://doi.org/10.1016/s0967-0645(99)00141-1

[23] Levitus, S. (1982) Climatological Atlas of the World Ocean. U.S. Department of Commerce, National Oceanic and Atmospheric Administration.

[24] Dilmahamod, A.F. (2014) Links between the Seychelles-Chagos Thermocline Ridge and Large Scale Climate Modes and Primary Productivity; and the Annual Cycle of Chlorophyll-a. http://hdl.handle.net/11427/9212

[25] Chatfield, C. and Xing, H. (2019) The Analysis of Time Series: An Introduction with R. 7th Edition, CRC Press.

[26] von Storch, H. and Zwiers, F.W. (2002) Statistical Analysis in Climate Research. Cambridge University Press.

[27] Martín-Rey, M., Polo, I., Rodríguez-Fonseca, B., Losada, T. and Lazar, A. (2018) Is There Evidence of Changes in Tropical Atlantic Variability Modes under AMO

Phases in the Observational Record? *Journal of Climate*, **31**, 515-536. https://doi.org/10.1175/jcli-d-16-0459.1

[28] Rodríguez-Fonseca, B., Polo, I., García-Serrano, J., Losada, T., Mohino, E., Mechoso, C.R., *et al.* (2009) Are Atlantic Niños Enhancing Pacific ENSO Events in Recent Decades? *Geophysical Research Letters*, **36**, L20705. https://doi.org/10.1029/2009gl040048

[29] Rodríguez-Fonseca, B., Janicot, S., Mohino, E., Losada, T., Bader, J., Caminade, C., *et al.* (2011) Interannual and Decadal SST-Forced Responses of the West African Monsoon. *Atmospheric Science Letters*, **12**, 67-74. https://doi.org/10.1002/asl.308

[30] Garratt, J. (1994) Review: The Atmospheric Boundary Layer. *Earth-Science Reviews*, **37**, 89-134. https://doi.org/10.1016/0012-8252(94)90026-4

[31] Stull, R.B. (2012) An Introduction to Boundary Layer Meteorology. Springer.

[32] de Szoeke, S.P., Fairall, C.W., Wolfe, D.E., Bariteau, L. and Zuidema, P. (2010) Surface Flux Observations on the Southeastern Tropical Pacific Ocean and Attribution of SST Errors in Coupled Ocean-atmosphere Models. *Journal of Climate*, **23**, 4152-4174. https://doi.org/10.1175/2010jcli3411.1

[33] de Boyer Montégut, C., Madec, G., Fischer, A.S., Lazar, A. and Iudicone, D. (2004) Mixed Layer Depth over the Global Ocean: An Examination of Profile Data and a Profile-Based Climatology. *Journal of Geophysical Research: Oceans*, **109**, C12003. https://doi.org/10.1029/2004jc002378

[34] Foltz, G.R., Schmid, C. and Lumpkin, R. (2013) Seasonal Cycle of the Mixed Layer Heat Budget in the Northeastern Tropical Atlantic Ocean. *Journal of Climate*, **26**, 8169-8188. https://doi.org/10.1175/jcli-d-13-00037.1

[35] Wang, C., Lee, S. and Mechoso, C.R. (2010) Interhemispheric Influence of the Atlantic Warm Pool on the Southeastern Pacific. *Journal of Climate*, **23**, 404-418. https://doi.org/10.1175/2009jcli3127.1

[36] Jouanno, J., Hernandez, O. and Sanchez-Gomez, E. (2017) Equatorial Atlantic Interannual Variability and Its Relation to Dynamic and Thermodynamic Processes. *Earth System Dynamics*, **8**, 1061-1069. https://doi.org/10.5194/esd-8-1061-2017

[37] Frankignoul, C. (1985) Sea Surface Temperature Anomalies, Planetary Waves, and Air-Sea Feedback in the Middle Latitudes. *Reviews of Geophysics*, **23**, 357-390. https://doi.org/10.1029/rg023i004p00357

[38] Xie, S. and Carton, J.A. (2004) Tropical Atlantic Variability: Patterns, Mechanisms, and Impacts. In: Wang, C., Xie, S.P. and Carton, J.A., Eds., *Earth's Climate: The Ocean-Atmosphere Interaction*, *Volume* 147, American Geophysical Union, 121-142. https://doi.org/10.1029/147gm07

[39] Wang, W. and McPhaden, M.J. (1999) The Surface-Layer Heat Balance in the Equatorial Pacific Ocean. Part I: Mean Seasonal Cycle. *Journal of Physical Oceanography*, **29**, 1812-1831. https://doi.org/10.1175/1520-0485(1999)029<1812:tslhbi>2.0.co;2

[40] Deser, C., Phillips, A.S. and Alexander, M.A. (2010) Twentieth Century Tropical Sea Surface Temperature Trends Revisited. *Geophysical Research Letters*, **37**, L10701. https://doi.org/10.1029/2010gl043321

[41] Trenberth, K.E. (1990) Recent Observed Interdecadal Climate Changes in the Northern Hemisphere. *Bulletin of the American Meteorological Society*, **71**, 988-993. https://doi.org/10.1175/1520-0477(1990)071<0988:roicci>2.0.co;2

[42] Yeh, S., Kug, J., Dewitte, B., Kwon, M., Kirtman, B.P. and Jin, F. (2009) El Niño in a Changing Climate. *Nature*, **461**, 511-514. https://doi.org/10.1038/nature08316

[43] Klein, S.A., Hartmann, D.L. and Norris, J.R. (1995) On the Relationships among Low-

Cloud Structure, Sea Surface Temperature, and Atmospheric Circulation in the Summertime Northeast Pacific. *Journal of Climate*, **8**, 1140-1155. https://doi.org/10.1175/1520-0442(1995)008<1140:otralc>2.0.co;2

[44] Tokinaga, H., Xie, S. and Mukougawa, H. (2017) Early 20th-Century Arctic Warming Intensified by Pacific and Atlantic Multidecadal Variability. *Proceedings of the National Academy of Sciences of the United States of America*, **114**, 6227-6232. https://doi.org/10.1073/pnas.1615880114

[45] Chiang, J.C.H. and Vimont, D.J. (2004) Analogous Pacific and Atlantic Meridional Modes of Tropical Atmosphere-Ocean Variability. *Journal of Climate*, **17**, 4143-4158. https://doi.org/10.1175/jcli4953.1

[46] Faye, S., Lazar, A., Sow, B.A. and Gaye, A.T. (2015) A Model Study of the Seasonality of Sea Surface Temperature and Circulation in the Atlantic North-Eastern Tropical Upwelling System. *Frontiers in Physics*, **3**, Article 76. https://doi.org/10.3389/fphy.2015.00076

[47] Worou, K., Goosse, H., Fichefet, T. and Kucharski, F. (2022) Weakened Impact of the Atlantic Niño on the Future Equatorial Atlantic and Guinea Coast Rainfall. *Earth System Dynamics*, **13**, 231-249. https://doi.org/10.5194/esd-13-231-2022

[48] Rodríguez-Fonseca, B., Mohino, E., Mechoso, C.R., Caminade, C., Biasutti, M., Gaetani, M., *et al.* (2015) Variability and Predictability of West African Droughts: A Review on the Role of Sea Surface Temperature Anomalies. *Journal of Climate*, **28**, 4034-4060. https://doi.org/10.1175/jcli-d-14-00130.1

[49] Casselman, J.W., Lübbecke, J.F., Bayr, T., Huo, W., Wahl, S. and Domeisen, D.I.V. (2023) The Teleconnection of Extreme El Niño-Southern Oscillation (ENSO) Events to the Tropical North Atlantic in Coupled Climate Models. *Weather and Climate Dynamics*, **4**, 471-487. https://doi.org/10.5194/wcd-4-471-2023

[50] Exarchou, E., Ortega, P., Rodríguez-Fonseca, B., Losada, T., Polo, I. and Prodhomme, C. (2021) Impact of Equatorial Atlantic Variability on ENSO Predictive Skill. *Nature Communications*, **12**, Article No. 1612. https://doi.org/10.1038/s41467-021-21857-2

[51] Carvalho, L.M.V., Jones, C., Cannon, F. and Norris, J. (2016) Intraseasonal-To-Interannual Variability of the Indian Monsoon Identified with the Large-Scale Index for the Indian Monsoon System (LIMs). *Journal of Climate*, **29**, 2941-2962. https://doi.org/10.1175/jcli-d-15-0423.1

[52] Thiam, M., Oruba, L., de Coetlogon, G., Wade, M., Diop, B. and Farota, A.K. (2024) Impact of the Sea Surface Temperature in the North-Eastern Tropical Atlantic on Precipitation over Senegal. *Journal of Geophysical Research: Atmospheres*, **129**, e2023JD040513. https://doi.org/10.1029/2023jd040513

[53] Sutton, R.T. and Hodson, D.L.R. (2003) Influence of the Ocean on North Atlantic Climate Variability 1871-1999. *Journal of Climate*, **16**, 3296-3313. https://doi.org/10.1175/1520-0442(2003)016<3296:iotoon>2.0.co;2

[54] Tamoffo, A.T., Weber, T., Mouassom, F.L., Le-Roy, B., Teichmann, C., Jacob, D., *et al.* (2025) The Global Sahel Monsoon Ocean-Pressure Index Reconciles Its Regional and Large-Scale Features. *npj Climate and Atmospheric Science*, **8**, Article No. 323. https://doi.org/10.1038/s41612-025-01226-2